Published in final edited form as:
Nat Struct Mol Biol. 2010 April ; 17(4): 430–437. doi:10.1038/nsmb.1780.

Dynamic changes in histone acetylation regulate origins of DNA replication

Ashwin Unnikrishnan[1,2], **Philip R. Gafken**[3], and **Toshio Tsukiyama**[1,*]

[1]Divison of Basic Sciences, Fred Hutchinson Cancer Research Center, 1100 Fairview Avenue North, Seattle, WA 98109, U.S.A.

[2]Molecular and Cellular Biology Program, Fred Hutchinson Cancer Research Center and University of Washington, Seattle, WA 98195, U.S.A.

[3]Proteomics Facility, Fred Hutchinson Cancer Research Center 1100 Fairview Avenue North, Seattle, WA 98109, U.S.A.

Abstract

While histone modifications have been implicated in many DNA-dependent processes, their precise role in DNA replication remains largely unknown. Here, we describe a very efficient, single-step method to specifically purify histones located around an origin of replication from *S. cerevisiae*. Using high-resolution mass spectrometry, we have obtained a comprehensive view of the histone modifications surrounding the origin of replication throughout the cell cycle. We have discovered that histone H3 and H4 acetylation is dynamically regulated around an origin of replication, at the level of multiply-acetylated histones. Furthermore, we find that this acetylation is required for efficient origin activation during S-phase.

Keywords

DNA replication; histone modifications; mass spectrometry

Eukaryotic DNA replication occurs in the context of chromatin. The fundamental unit of chromatin is the nucleosome, in which 147 base pairs of DNA tightly wrap around a histone octamer, consisting of the core histones H2A, H2B, H3 and H4[1]. The packaging of DNA into chromatin profoundly influences DNA-dependent processes such as transcription, replication, repair and recombination[2,3]. A large variety of covalent modifications are added to histones post-translationally, including acetylation, methylation, phosphorylation and ubiquitination, to influence DNA-dependent processes[4].

DNA replication occurs in the S-phase of the cell cycle and initiates at discrete sites on the chromosome called origins of replication (henceforth “origins”). DNA replication has been best studied in the budding yeast, *Saccharomyces cerevisiae*, where origins were first identified as autonomous replication sequence (ARS) elements in plasmid maintenance assays[5]. A number of protein complexes are assembled at an origin in a tightly regulated, temporally controlled manner over the cell cycle to initiate replication. Replication forks then travel bi-directionally outwards from the origin until the entire genome is replicated6.

*Corresponding author: ttsukiya@fhcrc.org.

AUTHOR CONTRIBUTIONS A.U. performed the experiments, with help by P.G. on MS analyses. T.T. supervised the experiments. A.U. and T.T. wrote the manuscript. All authors discussed the results and approved the manuscript.

It is thought that the accessibility of DNA to replication factors can be influenced by local chromatin structure[6,7,8]. Additionally, chromatin structure modulates origin firing time and efficiency, although the exact mechanisms are unknown[9,10]. The acetylation of the ε-amino group of a lysine residue on a histone protein neutralizes its positive, which is believed to create a more accessible chromatin structure, facilitating DNA-dependent processes. Supporting a role for histone acetylation in DNA replication, deletions of the Rpd3 histone deacetylase in *S. cerevisiae* advance the activation time of a subset of origins11,12. Conversely, artificial recruitment of the Gcn5/KAT2 histone acetyltransferase to the vicinity of a late-firing origin (ARS1412) advances the firing time of the origin12. Intriguingly, a mammalian-specific MYST-family histone acetyltransferase Hbo1 is found associated with Orc113 and Mcm214 in vivo. The NAD(+)-dependent histone deacetylase, Sir2, has been shown to repress the firing of origins in the ribosomal DNA cluster15 and of some chromosomal origins in *S. cerevisiae*[16].

Despite these links between histone modifications and DNA replication, the exact histone modifications involved in DNA replication remain largely unknown. There are two probable reasons: (i.) In most organisms apart from *S. cerevisiae*, it is hard to localize origins of replication to a small, well-defined region of DNA. In a number of organisms, origins have only been narrowed down to at most a few kilobases, which encompasses many nucleosomes. Even in *S. cerevisiae*, there are only 200–400 origins in the ~12.5Mb genome17,18, meaning that on average, there is one origin every 30kb. Since no origin is used in every cell cycle, histone modifications specifically associated with active origins will be sparsely distributed throughout the genome. These modifications will therefore be of low-abundance in a background of abundant modifications on genomic chromatin, and would likely remain undetected in analyses on bulk histones. (ii.) Most studies of histone modifications have been performed by chromatin immunoprecipitation (ChIP), which is a very useful tool in studying histone modifications. Yet, ChIP has some limitations as a tool for discovering new histone modifications or in studying combinations of modifications. ChIP requires a priori knowledge of the existence of modifications, since antibodies against the modifications have to be generated. Many of the modified residues on histones are often clustered close together, especially at the amino-terminus, and may act in combination to regulate DNA-dependent processes. Given the large number of modifications, it is becoming increasingly difficult to raise specific antibodies against all combinations of modifications. The binding of antibodies to their epitopes can be blocked by nearby modifications, and antibodies raised against single modifications can recognize different populations of histones to those raised against combinations of the modifications[19].

Here, we describe the development of a method to very efficiently purify histones specifically from a region flanking an active origin, enabling the detection of histone modifications by high-resolution mass spectrometry. Using this system, we have comprehensively identified histone modifications, some of which were detected only around the origin and/or in specific stages of the cell cycle. By quantitatively analyzing histone acetylation, we uncover the dynamic regulation of histones H3 and H4 amino-terminal acetylation, uniquely around ARS1, operating specifically at the level of multiply-acetylated histones. Importantly, we find that that this histone acetylation facilitates firing of endogenous origins at chromosomal locations.

Results

To elucidate how histone modifications affect DNA replication, we first sought to identify modifications that are present around an origin throughout the cell cycle, in a comprehensive and unbiased manner.

We decided to use tandem mass spectrometry (MS) to identify histone modifications. MS is a powerful tool to identify new histone modifications[20,21]. MS does not require *a priori* knowledge of the existence of the modification and can detect modifications of residues buried within the nuclesome core[22]. Importantly, MS is also able to detect combinations of modifications present on the same peptide[23]. However, thus far, MS has only been applied to study modifications on bulk histones purified from the entire genome, since there are no currently available techniques to purify histones, with enough quality and quantity, from specific chromosomal regions.

Development of the TRP1-ARS1-LacO minichromosome

Histones purified from a small minichromosome are suitable for studying how histone modifications change around an origin throughout the cell cycle. As described above, replication-associated histone modifications may be in low-abundance in bulk histones. The small number of nucleosomes per minichromosome means that each nucleosome is in close proximity to the origin, increasing the chance of identifying modifications specifically enriched in a region of active replication. The TRP1-ARS1-LacO minichromosome (Fig 1a) is derived from a 1.45 kb EcoRI fragment of the yeast genome that contains the *TRP1* gene and an early firing, efficient origin, ARS124. Nucleosome mapping revealed that the TRP1-ARS1 minichromosome contains seven nucleosomes[25]. Simpson and colleagues isolated minichromosomes away from yeast genomic DNA by utilizing a modified TRP1-ARS1 containing a single copy of the prokaryotic lac operator (lacO) sequence inserted into ARS1[26,27]. The minichromosome was affinity-purified from whole cell extracts using immobilized lac repressor26. A similar system utilizing tet-repressor has also been described28.

To enable the comprehensive identification of histone modifications, a high coverage of all the histones was essential, for which about 50–100 ng per core histone was needed (data not shown). However, the existing minichromosome purification methods do not provide sufficient quantity or quality of samples. We therefore needed a substantial improvement in both yield and purity of minichromosomes. We achieved this by optimizing multiple steps of the minichromosome purification protocol as schematized in Fig 1b (see Methods for details).

These modifications dramatically improved the purity and the yield of the template, allowing us to obtain 1–2 μg of total histones from a 10 liter of early log phase culture (~4×10^{10} cells). If average 50 copies of TALO8 exist per cell, this means about 40% of histones were recovered from TALO8. Given the relative enrichment of histones and the purity of the samples (Fig 1c), we were able to perform MS directly following affinity-purification of TALO8. This enabled us to attain 85–95% coverage of the four core histones (Supplementary Figure 1). The majority of the undetected peptides were too small owing to the close proximity of Arginine-C (ArgC) cleavage sites, illustrating that we identify the vast majority of analyzable histone peptides.

To analyze MS data, we used an open-source program, X!Tandem[29]. X!Tandem was run in a refinement search mode, searching for eight modifications – lysine (K) acetylation, lysine mono-, di- or tri-methylation, lysine mono-ubiquitylation, arginine (R) mono- or di-methylation and serine (S) phosphorylation – in all possible combinations (see Methods for details). The top candidates were then manually verified (Supplementary Figure 2).

Identification of histone modifications around an origin

We hypothesized that good candidates for histone modifications involved in DNA replication would exhibit cell-cycle specific changes in abundance, and/or be specifically

enriched on TALO8, as compared to bulk chromatin. We therefore affinity-purified TALO8 from asynchronously growing cells, from cells arrested in G1-phase with α-factor, and from cells synchronously released from α-factor arrest and harvested in either S-phase or G2/M (Supplementary Figure 1a, see Methods for details). The S-phase time point for harvesting cells was determined by 2-D agarose gel electrophoresis[30], which revealed that the firing of ARS1 origin on TALO8 was detected 17 minutes after release (data not shown). G2/M was taken at 60 minutes after release, at which point the entire genome had been replicated as determined by flow cytometry (Supplementary Figure 1). As a control, and to gauge the general level of histone modifications in the entire genome, we purified bulk, chromatin-bound histones from isogenic cells lacking TALO8 harvested in each of the corresponding cell cycle stages.

We were able to detect a large number of histone modifications with a very high degree of confidence, including previously unknown modifications (Supplementary Figure 1c). Representative examples of the high-quality data obtained are shown for several modified histone peptides that are relevant to our analyses (Supplementary Figure 3). The MS data for other peptides are available upon request. A number of histone modifications are detected on both TALO8-purified and bulk histones, while mono-methylation of H2B K111 is only seen on bulk histones. Some modifications also show cell cycle variation. For example, H3 K37 mono-methylation is observed in G1 and G2/M-phases but undetectable in S-phase, while H4 K79 acetylation is detected in S- and G2/M-phases but not in G1.

Interestingly, a handful of modifications are exclusively identified on TALO8-purified histones, such as H2A S15 phosphorylation, H4 K79 acetylation and H3 K37 monomethylation (Supplementary Figure 1c). This suggests the possibility that these modifications specifically occur in regions close to origins.

Detection of combinations of histone modifications around an origin

A major advantage of MS is the ability to detect combinations of multiple histone modifications on the same molecule, when the modifications are closely clustered. The amino-terminal tails of histones H3 and H4 have a large number of modifiable residues, many of which are in close proximity. We therefore reasoned that our MS data might reveal previously unidentified patterns in histone modification combinations.

A number of modification combinations are identified on histones on TALO8, including di-acetylations on the amino-terminal of H3 and all combinations of acetylations of the H4 amino-terminal tail (Fig 2), as previously reported[23,31]. The combinations of H3 and H4 amino-terminal acetylations were detected on both TALO8 and bulk histones in all cell cycle stages. The peptide containing H3 K27 and K36 (K^{27}SAPSTGGV$K^{36}K^{37}$PHR) enabled an investigation of the interplay between H3 K27 acetylation and H3 K36 methylation. H3 K27 is acetylated by the Gcn5/KAT2 lysine acetyltransferase and shows a general enrichment in transcriptionally active regions[32]. H3 K36 is methylated by the Set2/KMT3 lysine methyltransferase[33], enriched throughout the coding region of open reading frames[34] and is involved in suppressing cryptic transcription within ORFs[35]. Intriguingly, specifically on TALO8, H3 K27 acetylation is always uniquely found in combination with tri-methylated H3 K36 and not with any other states of K36 methylation (Fig 2). On the other hand, TALO8-associated histone H3 containing monomethylated or di-methylated H3 K36 all lacked H3 K27 acetylation on the same histone.

Additionally, mono-methylated H3 K37, which is a TALO8 specific histone modification, is always detected in combination with mono-methylated H3 K36 (Fig 2). In contrast, we detect peptides where H3 K36 alone is mono-methylated, suggesting that H3 K37 mono-

methylation always happens in the context of mono-methylated H3 K36, whereas H3 K36 mono-methylation does not require a modified H3 K37.

Quantitative analysis of histone acetylations around an origin

The acetylation of lysine residues is one of the most intensively studied modifications on histones. The acetylation of H3 K56 increases specifically in S-phase and has been implicated in DNA replication and the intra S-phase checkpoint[36–39]. While H4 amino terminal acetylations have also been implicated in S-phase[40,41], neither the exact combinations of lysine residues nor the quantity of H4 acetylation around origins of replication is known.

We sought to address this important question by taking advantage of the TALO8 system. Histones were purified from TALO8 and bulk chromatin over the course of a cell cycle. The histones were then *in vitro* acetylated using deuterated (d6 -) acetic anhydride, converting all unmodified lysines into d6-acetyl-lysines[42] (see Methods for detail). This allowed for the quantitation of acetylations by comparing the abundance of protiated to deuterated peptides of interest (schematized in Supplementary Fig 4).

The MS analyses enabled the quantitative study of histone acetylations at individual lysine residues on histones H3 and H4 without consideration of the acetylation states of other lysines on the same peptide, as well as to examine the changes in combinations of acetylations on the same peptide.

We first examined the changes in H3 K56 acetylation since this is a well-studied S-phase enriched modification[37]. Consistent with a role as a mark on newly deposited histones, H3 K56 acetylation levels increased sharply from G1 into S-phase (17 minutes after release from α-factor), rising to 40% on TALO8-associated histones and 56.3% on bulk histones (Fig 3a, b). Consistent with the action of the histone deacetylases Hst3 and Hst4 on H3 K56 outside of S-phase[38], we find that H3 K56 acetylations levels are substantially decreased in G1 (Fig 3a, b). Importantly, the pattern of dynamic changes in H3 K56 acetylation is very similar on TALO8 and bulk chromatin, suggesting that it is regulated similarly irrespective of proximity to origins.

Unexpectedly, the pattern of acetylations on the histone H4 amino-terminal is markedly different on TALO8 compared to bulk, chromatin-bound histones. On bulk histones, the acetylation levels do not vary greatly throughout the cell cycle at any single residue (Fig 3b). Most of the acetylated H4 on bulk histones are mono-acetylated, remaining ~40% throughout the cell cycle (Fig 3). A large proportion of the mono-acetylated H4 in bulk chromatin can be attributed to mono-acetylation at K16, which stays ~50% (Fig 4b). The high abundance of H4 K16 acetylation is a likely reflection of the general euchromatic nature of the *S. cerevisiae* genome, since H4 K16 acetylation by Sas2 counteracts SIR-mediated silencing in *S. cerevisiae*[43,44].

On TALO8, however, the pattern of histone acetylation is strikingly different from bulk. The level of H4 acetylation is generally low in G1 and greatly increased in S-phase (Fig 3a, c). The acetylation levels of all four lysines on TALO8 are highest in asynchronously growing cells. Given that ~60% of the cells in an asynchronously growing culture of cells are in G2/M (see asynchronous flow cytometry profile in Supplementary Figure 1a), the highest levels of acetylation observed in asynchronous cells can be attributed to increased acetylation levels in G2/M. We observe a dramatic increase in the fraction of multiply acetylated H4 specifically on TALO8 (Fig 3c), with tetra-acetylated H4 increasing ~42 fold (from 0.08% in G1 to 3.4% in S-phase) and tri-acetylated H4 increasing ~11 fold in the same stage. The proportion of these species increases further in G2/M, reflected by their greater abundance

in asynchronously growing cells. At the same time, the level of mono-acetylated H4 remains relatively constant throughout the cell cycle (Fig 3c). This therefore means that the large increase in H4 acetylation on TALO8 in S-phase and G2/M is primarily due to the increase in the fraction of H4 tail with multiple acetylations on the same peptide. At the same time, our data reveals a sharp wave of histone H4 deacetylation specifically around ARS1 (Fig 3a, c), as cells progress from G2/M into G1. Furthermore, given that the fraction of mono-acetylated H4 on TALO8 remains constant throughout the cell cycle, the main function of this wave of deacetylation is to decrease the amount of multiply acetylated histone H4 specifically around the origin. The trends are similar for acetylations on the histone H3 amino-terminal, although the changes are not as dramatic as H4.

Multiple acetylations of H3 and H4 tails are required for efficient DNA replication

To determine if the increase in multiply-acetylated H3 and H4 play a functional role in DNA replication, we systemically tested combinational mutations of acetylatable lysine residues on H3 and H4 amino-terminal tails in yeast cells where the mutant histone was the only source (see Methods for details). None of the single or double lysine to arginine (K to R) mutants of either H3 or H4 alone conferred any substantial growth defects (Supplementary Figure 5). Strikingly, however, when a triple K to R mutation of histone H4 (H4 K5,8,12R or H4 K5,12,16R) was combined with H3 mutations (H3 K9,14R or H3 K18,23,27R), the cells exhibited a marked growth defect on rich media (YPD). The mutants grew very slowly at room temperature and 30 °C and died at 37°C. Furthermore, cells with fewer mutations on acetylatable lysine residues on H3 and H4 tails show substantially weaker growth defects (Supplementary Figure 5a). These results show that the number of acetylatable lysine residues on H3 and H4 tails is inversely correlated with the severity of the growth defect.

To determine if the cells are impaired in DNA replication, we tested their sensitivity to replication inhibitors hydroxyurea (HU), methylmethane sulfonate (MMS) and camptothecin. The H3 K9,14R/H4 K5,8,12R mutant is extremely sensitive to all three classes of replication inhibitors (Fig 4 a, b). However, unlike a *mec1 sml1* checkpoint mutant, the histone mutant is not sensitive to other forms of DNA damage, such as UV-or γ-irradiation (Fig 4b), indicating that this mutant is not defective in general DNA-damage response. Histone mutants with larger numbers of remaining acetylatable lysine residues on H3 and H4 tails exhibit notably less sensitivity to replication inhibitors (Supplementary Figure 5a).

To directly test whether the histone mutant exhibits a replication defect, we pre-synchronized cells in G1 with α-factor and monitored cell cycle progression in rich media (YPD) by flow cytometry. Two major defects can be observed in the histone mutant. Firstly, it takes a substantially longer time for detectable genomic DNA replication to begin in the histone mutant (60 minutes after release from G1 arrest) compared to wild type cells which have progressed well into S-phase by 40 minutes (Fig 4c). Secondly, the histone mutant takes twice as long to complete DNA replication (40 ~50 minutes) compared to wild type cells (~20 minutes, Fig 4c). Since the histone mutant only exhibits a 5 minute delay in budding compared to wild type cells upon release from α-factor, the slower S-phase progression is largely due to impaired DNA replication. In contrast, a histone mutant that lacks four acetylatable lysine residues (H3 Δ9–14/H4 K5,12R) instead of five (H3 K9,14R/H4 K5,8,12R) did not exhibit a notable delay in S phase progression in rich media (YPD), and showed only a slight delay in S phase progression in the presence of 50 mM HU (Supplementary Figure 5c). These results strongly support our model that acetylation of multiple lysine residues on H3 and H4 tails play critical roles in DNA replication. Because of its strong replication defects, we used the H3 K9,14R/H4 K5,8,12R quintuple mutant (hereafter “histone acetylation mutant”) for further analyses.

H3 and H4 acetylations are necessary for efficient origin firing

The increase in H3 and H4 tail acetylations in S and G2/M phases occurs specifically on TALO8. This suggested that the H3/H4 acetylations have a unique role pertaining to origin activity and that the replication defects observed in our histone mutant might be due to impaired origin function.

The plasmid loss assay is a quick and sensitive means to identify defects in DNA replication[45]. We tested plasmids harboring either ARS1 or a late-firing origin, ARS1413, and detected elevated plasmid loss rates for both plasmids in the histone mutant (data not shown). If elevated plasmid loss rate is due to reduced efficiency of origin firing, then having multiple origins on a plasmid is expected to at least partially reduce the loss rate in the histone acetylation mutant[46]. As shown in Figure 5a, the presence of multiple origins does not significantly affect the loss rate in wild type cells. In sharp contrast, an elevated loss rate of a plasmid containing only one functional origin in the histone acetylation mutant is significantly reduced in the presence of eight functional origins (Fig 5a). This result strongly suggests that the elevated plasmid loss rates in the histone acetylation mutant are largely due to origin firing defects. These results, however, do not exclude the possibility that H3 and H4 acetylation affects other steps in DNA replication.

To confirm the origin firing defects at chromosomal locations in the histone acetylation mutant, we performed two-dimensional (2-D) agarose gel electrophoresis analysis[30]. Because the histone mutant and wild type cells have dramatically different cell cycle progression rates (Fig 4c), we first blocked cells in S-phase by releasing α-factor arrested cells into HU. Consistent with our interpretation of the FACS profiles in Fig 4c, the appearance of “bubble” structures associated with an active ARS1 origin at its chromosomal location is delayed in the histone mutant compared (Fig 5b). Furthermore, the intensity of the bubble arc is dramatically weaker than in wild type (~8-fold difference, Fig 5b). Bubble structures at another early origin, ARS 607, at its chromosomal location were also reduced in the histone mutant (~5-fold difference, Fig 5c).

A similar reduction in bubble structures was observed in the histone mutant during unperturbed growth. We performed 2-D gel analyses on pooled S-phase population of cells (see Methods). Once again, the intensity of bubble structures at ARS1 and ARS 607 are weaker in the histone mutant (Fig 6a). Furthermore, we observed similar, albeit less dramatic, decrease in origin firing of ARS501, a late-firing origin (Fig 6b). These results strongly support our conclusion that acetylation of multiple lysine residues on H3 and H4 tails is necessary for efficient firing of replication origins.

Discussion

TALO8 is a powerful tool for studying site-specific chromatin events in vivo

We have developed an extremely efficient system to specifically purify histones located around an origin in a single step. Using this system, we report the first comprehensive identification of the histone modifications around an origin through the cell cycle. To our knowledge, this is the first application of mass spectrometry to identify combinations of histone modifications present in a specific region of the genome.

The utility of TALO8 extends beyond studying histone modifications. In this study, despite optimizing the protocol for histone purification by utilizing stringent washes, we have detected a number of other chromatin-bound proteins (Supplementary Table 1). Subunits of the Minichomosome Maintenance (MCM) complex and the Origin Recognition Complex (ORC), which are involved in DNA replication were more abundant in S-phase cells on TALO8 (Supplementary Table 2).

By optimizing the affinity-purification protocol, TALO8 or its derivatives can be used to selectively purify and study any DNA-dependent processes that take place on the minichromosome. For example, the scheme could be adapted to identify chromatin-binding factors around a region of double-strand break, and to determine the post-translational modifications of those proteins concurrently. Alternatively, as illustrated by Akiyoshi et al[47], a centromere-containing TALO8 derivative can also be used to identify components of the kinetochore. Furthermore, the efficient purification of TALO8 and its associated proteins makes it an excellent substrate for *in vitro* biochemical assays. For example, TALO8 could be purified from mutants of transcription factors or chromatin modifying proteins to be used as a template in transcription assays *in vitro*. Finally, the purity and yield of the TALO8 also makes it ideal for electron microscopic observations of specific chromatin structures, such as stalled or collapsed replication forks in TALO8-containing cells defective in the replication checkpoint, or to directly visualize defective nucleosome assembly by purifying TALO8 from chromatin assembly mutants.

Apart from the dynamic pattern of H3 and H4 acetylations around an origin, we have also discovered a few modifications previously uncharacterized in *S. cerevisiae*, including the H2A S15 phosphorylation (located within the amino-terminal tail) and H2B K111 monomethylation (located on the surface of the nucleosome). We report the detection of acetylation on H4 K79 (located on the surface of the nucleosome), previously reported in calf thymus histones21 and for which a role in telomeric and ribosomal DNA silencing had been suggested from genetic analyses48. Furthermore, we detect a unique pattern of H2B K123 mono-ubiquitination on TALO8, which is implicated in nucleosome dynamics49,50. Another interesting modification we have detected is H3 K37 mono-methylation (located on the amino-terminal tail), specifically on TALO8, which is absent during S-phase (Supplementary Figure 1c). Mono-methylated H3 K36, along with histone acetylation, facilitates the loading of Cdc45 onto early origins[51]. It is therefore possible that mono-methylation of an adjacent residue H3 K37, specifically around an origin and outside of S-phase, might serve to prevent improper recruitment of Cdc45.

The binding of the tetracyclin repressor on a 10kb tandem array of operator sequence on a plasmid can stall replication forks in *E. coli*[52] and we cannot exclude the possibility that the binding of LacI onto the eight copies of *LacO* on TALO8 *in vivo* might also affect its replication. Similarly, although we prepared whole cell extracts to isolate TALO8 and bulk chromatin from the same stages of the cell cycle in identical fashion, we cannot exclude the possibility that the difference in the histone isolation methods made some contributions to the differences in histone modifications found on TALO8 and bulk chromatin. However, we do believe these factors have no major effects on histone modifications, as H3 K56 acetylation dynamics on TALO8 and in bulk chromatin were identical and exactly as expected from the nature of this modification (Fig 3), while acetylation on multiple lysine residues on H3 and H4 tails that are detected on TALO8 was shown to play critical roles in functions of chromosomal origins. In addition, we did not detect phosphorylation of H2A serine 129, which takes place at the sites of DNA damage, on TALO8.

Acetylated histones H3 and H4 regulate origin activity

By utilizing the TALO8 system, we have identified a unique pattern of acetylations specifically on histones flanking an origin of DNA replication. Our analyses have revealed that the two classes of histone acetylations implicated in DNA replication, one on H3 K56 and the other on the amino terminals of histones H3 and H4, are dynamically regulated in markedly distinct ways throughout the cell cycle. H3 K56 acetylation patterns are similar on TALO8 and bulk histones, increasing from low levels in G1 to high levels in S-phase before dropping again, as anticipated for a mark of histone deposition occurring behind a replication fork.

Histone H3 and H4 acetylation patterns, on the other hand, are dramatically different around an origin of replication compared to bulk. While remaining relatively constant on bulk histones, the levels of multiply acetylated H3 and H4 sharply increases on TALO8 in S-phase and G2/M around ARS1 before decreasing in G1. Based on these results, we propose that acetylation of H3 and H4 tails plays critical roles in the function of replication origins. The data from our plasmid loss assay (Fig 5a) and 2-D gel analyses of chromosomal origins (Figs 5b, c, 6) strongly supported our model. To our knowledge, this is the first report of the dynamic regulation of histone acetylation operating specifically at the level of multiple acetylations on the same histone molecule. The use of TALO8 to specifically purify origin-proximal histones and application of MS to detect histone modifications has enabled us to discover this pattern.

Given that the acetylation of H3 and H4 tails can also affect transcription of genes[3], we cannot exclude the possibility that some of the phenotypes of the histone acetylation mutant are due to indirect (transcriptional) effect of the mutations. However, because a dramatic increase in acetylation of multiple lysine residues on H3 and H4 tails in S and G2/M phases was observed only on histones in close proximity to ARS1 on TALO8 but not on bulk chromatin that represent genome-wide average, we favor a model that H3 and H4 tail acetylation directly facilitate origin firing.

Mutations of all the amino-terminal lysines of histone H4 have been shown to increase the lengths of S-phase and G2/M40·41 while simultaneously deleting large portions of the amino terminals of histones H3 and H4 cause cell death and accumulation in G2/M[53]. Yet, the exact molecular steps that were affected by these mutations had not been defined. Our data suggests that the acetylation of histones H3 and H4 around origins is required for efficient origin firing in unperturbed growth and becomes essential during replication stress. It is possible that an increased level of H3 and H4 acetylation facilitates the loading of replication factor(s) at origins. Alternatively, H3 and H4 tail acetylation might be required for DNA polymerases to initiate bidirectional progression from origins. We also speculate that the wave of deacetylation prior to the following G1 may enforce temporally controlled loading of those factors.

METHODS

Yeast strains

All yeast strains were grown and manipulated according to standard procedures. Supplemental Table 3 lists all the strains used in this study. All the yeast strains used in this study are derived from a W303 background in which a weak *rad5* mutant allele in the original W303-1a strain has been corrected[54,55]. Cells containing TALO8 were grown in selective synthetic media lacking tryptophan. Histone mutants were made in strains where both endogenous copies of histones H3 and H4 had been deleted, and covered with a URA3-marked, centromeric plasmid containing a wild type allele of H3 and H4. Plasmids containing a single copy of the mutated histones were integrated at the *TRP1* locus, verified by southern blotting to ensure that only a single copy of the plasmid was integrated, and then the plasmid containing wild type histone was shuffled out by counter-selection on 5-Fluoroorotic Acid (5-FOA). PCR was used to verify to that the mutant histone was the only version of histone gene present in the cell after plasmid shuffling. Histone mutations were created by site-directed mutagenesis (QuikChange kit, Stratagene).

Yeast growth and cell synchronization

All cells were grown at 30°C unless otherwise noted. Cells for arrest and release experiments were grown to an optical density of 0.20 – 0.25 at 660nm (OD660) in synthetic

media lacking tryptophan (YC - Trp) and arrested in G1-phase with 5 μg ml^{-1} α-factor for 90 minutes. Cells were released from G1-arrest by filtration on 0.45 μm nitrocellulose membranes (Millipore), washed and resuspended in fresh, pre-warmed media lacking α-factor. Cell synchrony was followed by flow cytometry[56]. Five-fold serial dilutions were performed on YPD agar plates (with or without appropriate drugs) and cells were grown for 3 days. Plates containing drugs were used within 24 hours of preparation.

Affinity-purification of TALO8

TALO8-containing cells were quickly killed at a specific cell cycle stage by vigorously mixing cultures with a frozen solution of 0.1M EDTA, pH 8.0 (to a final concentration of 17mM) and 0.1% Sodium Azide (Sigma). Cells were then spun down, washed once in twenty-fold cell pellet volume of water containing 2mM phenylmethanesulfonyl fluoride (PMSF) and then once in ten-fold cell pellet volume of Buffer H 150 [BH 150: 25mM HEPES-KOH pH 7.6, 2mM $MgCl_2$, 0.5mM EGTA, 0.1mM EDTA, 10% (v/v) glycerol, 150mM KCl, 0.02% (v/v) NP40] containing protease inhibitors [1mM PMSF, 2μM pepstatin, 600nM leupeptin, 2mM benzamidine, 2μg ml^{-1} chymostatin A (Sigma)], phosphatase inhibitors [2mM imidazole, 1mM sodium fluoride, 1.15mM sodium molybdate, 1mM sodium orthovanadate, 4mM sodium tartarate dihydrate, 2.5μM (−)-p-bromotetramisole oxalate, 0.5μM cantharidin, 0.5nM microcystin, (Sigma)] and histone deacetylase inhibitors [0.5μM Trichostatin A (Sigma), 25μM Sirtinol (Calbiochem)]. All the buffers in the following steps were kept on ice and supplemented with the inhibitors described above, unless otherwise specified. Whole cell extracts were made by bead beating cells resuspended in an equal volume of BH 150. The whole cell extracts were then centrifuged in a Beckman SW40Ti rotor at 27,000 rpm for 90 minutes at 4°C. The soluble extract was isolated and incubated with magnetic beads (Protein G Dynal beads, Invitrogen) crosslinked with anti-FLAG M2 antibody (Sigma) for 3 hours at 4°C. Typically, per ~ 4×10^9 cell equivalents of extract, 25 μl of Protein G beads slurry and 11.5 μg of anti-FLAG M2 antibodies were used. After the incubation, the magnetic beads were rinsed three times with BH 150 and then washed four times, 5 minutes per wash, in BH 300 (which was identical to BH 150, except containing 300mM KCl). The beads were then rinsed three times in Rinse Buffer [25mM HEPES KOH pH 7.6, 2mM MgCl2, 10% (v/v) glycerol, 150mM KCl, no inhibitors] and then four sequential elutions were performed, for 30 minutes each, at room temperature with Elution Buffer [50mM ammonium bicarbonate, 0.1% (w/v) Rapigest (Waters), no inhibitors]. The eluates were pooled, digested overnight with 100 ng of endoproteinase Arginine-C (Roche) at 37°C, trifluoroacetic acid was added to a final concentration 0.5% and incubated at 37°C for 1 hour to degrade Rapigest. The resulting solution was dried in a SpeedVac, resuspended in 0.1% (v/v) formic acid and loaded onto the mass spectrometer.

To prepare bulk, chromatin-bound histones, 2 ~ 4×10^8 cells (at OD660 = 0.2–0.25) were harvested from different cell cycle stages as described above. The cells were washed as above and lysed by bead beating in BH 150 supplemented with inhibitors, as described above. Soluble chromatin was prepared by sonication and incubated with Source 15Q (GE Healthcare) anion exchange beads for 20 minutes at 4°C. The beads were then washed twice with BH 250 (250mM KCl) and twice with BH 500 (500mM KCl), for 5 minutes per wash at 4°C. Core histones were then eluted in 2M KCl, digested overnight with 100 ng of Arg-C at 37°C, desalted using ZipTip C18 columns (Millipore) and analyzed on the mass spectrometer. All the buffers were kept chilled on ice and supplemented with inhibitors, unless otherwise specified.

Protein and Modification Identification

All the data were gathered by using liquid chromatography coupled in-line with electrospray ionization tandem mass spectrometry (LC-ESI MS/MS). This setup consisted of an Eksigent Technologies 2D nanoLC coupled to 75 μm × 20 cm analytical column made from a New Objective PicoFrit packed with 5 μm, 100 Å particle MAGIC C18AQ packing material and directly spraying into a Thermo-Scientific LTQ Orbitrap XL hybrid mass spectrometer via the mass spectrometer's nanospray ionization source. Chromatographic elution was performed at 500 nL/min using a 60 minute gradient from 2% solvent B to 50% solvent B, where solvent A was 0.1% (v/v) formic acid in water and solvent B was 0.1% (v/v) formic acid in acetonitrile, and a spray voltage of 2800 volts was applied to the electrospray tip. The mass spectrometer was operated in the "shotgun" mode for MS/MS acquisitions. Here, an MS survey scan was performed in the OrbiTrap portion of the instrument (AGC target value 1e6, resolution 60K, and injection time 150 ms) and tandem MS (MS/MS) fragmentation scans on the top five abundant ions from the survey scan were performed in the ion trap portion of the instrument (normalized collision energy of 35%; isolation width of 2 m/z; target value of 1e4; injection time of 100 ms). Selected ions were dynamically excluded for 45 seconds with a repeat count of 1. The precursor ion selection for MS/MS was set to +/− 0.5 Da (parent mass width) and charge state screening was enabled allowing only +2 and +3 charged peptides to be selected for MS/MS.

Protein and modification identification were performed by analyzing mass spectrometry data with the protein database search algorithm X!Tandem used in the refinement mode. The following variable mass modifications were used: 14.015 Da and 28.031 Da for mono- and dimethylation on lysine respectively, 42.047 Da for trimethylation on lysine, 42.011 Da for acetylation on lysine, 114.043 for ubiquitination on lysine, 15.995 for oxidation on methionine, and 79.966 for phosphorylation on serine. The Saccharomyces Genome Database was used as the reference protein database with the addition of human keratins and Lac repressor protein sequences to account for potential contaminating proteins. The score function of native X!Tandem was replaced with a dot-product based scoring algorithm that is compatible with Peptide Prophet[57]. Peptide identifications results were filtered and sorted in CPAS[58] using parameters that result in a false discovery rate of 5% or less, before being manually verified. Detection of all the modifications, including quantitative analysis of acetylation, is based on 20–50 peptides per modification. The MS-MS data of relevant modified histone peptides are shown in Supplemental Figure 2. The MS-MS data for other modified histone peptides are available upon request.

Acetylation Quantitation

For the quantitation of acetylation by mass spectrometry, TALO8 (or bulk histones) was eluted as per normal and the histones were precipitated using 20% (w/v) Trichloroacetic acid (Sigma). The dried eluates were then acetylated *in vitro*, digested overnight with Arg-C at 37°C and the data analyzed as described in (Smith et al., 2003), but with the following modification: the *in vitro* acetylation was performed in a solution of 5% (v/v) triethylamine, 5% (v/v) d6-acetic anhydride and acetonitrile for 1 hour at room temperature. Mass spectrometry was performed in an identical fashion as described above for modification identification, except that the dynamic exclusion function was not utilized. The precursor ion selection for MS/MS was set to +/− 4.5 Da, and an inclusion list of ions selected for MS/MS quantitation were 494.77, 530.31, 639.62 and 722.405. We performed the analysis in duplicate, and the results were essentially identical.

Two-dimensional gel electrophoresis and hybridization

Cells were arrested with EDTA and sodium azide, as previously described for TALO8. Total genomic DNA was prepared according to the "CTAB extraction" procedure[59,60]. To prepare

pooled fraction of S-phase cells, equal volumes of cells were harvested at designated intervals that spanned the entirety of S-phase for both wild type and histone mutant, arrested with EDTA and sodium azide, pooled and total genomic DNA was harvested. 5μg of DNA was digested with either *Nco*I (ARS1), *BspH*I and *Cla*I (ARS607) or *Xba*I (ARS501) and 2-D gels were performed as originally described[30]. The DNA was blotted onto Nylon GeneScreen Plus membranes (PerkinElmer) and separately probed with ^{32}P-labelled DNA probes spanning each respective ARS. Probes were amplified from yeast genomic DNA by PCR and gel purified (sequences available upon request). Signals were quantified on a Phosphorimager (GE Healthcare) and ImageQuant, as described[64]. The values are reported as a percentage of the intensity of the 1N linear spot. All enzymes used in this paper were purchased from New England Bio labs.

Supplementary Material

Refer to Web version on PubMed Central for supplementary material.

Acknowledgments

We are especially grateful to Sue Biggins, Bungo Akiyoshi and Noelle Ebel for technical help and advice in developing the TALO8 purification scheme. We thank Lisa Nader Jones and Jason Hogan of the Proteomics Facility at the FHCRC for help with MS, and Jimmy Eng and Brendan MacLean for advice with using X!Tandem. We thank Tracey Kwong (FHCRC), Doug Koshland (Carnegie Institute), Bonita Brewer and M. K. Raghuraman (University of Washington) for the plasmids used in the plasmid loss assay. We also thank members of the Tsukiyama lab, Susan Parkhurst, Sue Biggins, Bungo Akiyoshi and Christian Nelson for helpful comments with the manuscript. This work is supported in part by NIH grant R01 GM078259 to TT. The FHCRC Proteomics Facility is supported by cancer center support grant P30 CA15704.

References

1. Luger K, Mader AW, Richmond RK, Sargent DF, Richmond TJ. Crystal structure of the nucleosome core particle at 2.8 A resolution. Nature. 1997; 389:251–60. see comments. [PubMed: 9305837]
2. Groth A, Rocha W, Verreault A, Almouzni G. Chromatin challenges during DNA replication and repair. Cell. 2007; 128:721–33. [PubMed: 17320509]
3. Li B, Carey M, Workman JL. The role of chromatin during transcription. Cell. 2007; 128:707–19. [PubMed: 17320508]
4. Kouzarides T. Chromatin modifications and their function. Cell. 2007; 128:693–705. [PubMed: 17320507]
5. Stinchcomb DT, Struhl K, Davis RW. Isolation and characterisation of a yeast chromosomal replicator. Nature. 1979; 282:39–43. [PubMed: 388229]
6. Bell SP, Dutta A. DNA replication in eukaryotic cells. Annu Rev Biochem. 2002; 71:333–74. [PubMed: 12045100]
7. Brown JA, Holmes SG, Smith MM. The chromatin structure of Saccharomyces cerevisiae autonomously replicating sequences changes during the cell division cycle. Mol Cell Biol. 1991; 11:5301–11. [PubMed: 1922046]
8. Simpson RT. Nucleosome positioning can affect the function of a cis-acting DNA element in vivo. Nature. 1990; 343:387–9. [PubMed: 2405281]
9. Ferguson BM, Fangman WL. A position effect on the time of replication origin activation in yeast. Cell. 1992; 68:333–9. [PubMed: 1733502]
10. Stevenson JB, Gottschling DE. Telomeric chromatin modulates replication timing near chromosome ends. Genes Dev. 1999; 13:146–51. [PubMed: 9925638]
11. Aparicio JG, Viggiani CJ, Gibson DG, Aparicio OM. The Rpd3-Sin3 histone deacetylase regulates replication timing and enables intra-S origin control in Saccharomyces cerevisiae. Mol Cell Biol. 2004; 24:4769–80. [PubMed: 15143171]

12. Vogelauer M, Rubbi L, Lucas I, Brewer BJ, Grunstein M. Histone acetylation regulates the time of replication origin firing. Mol Cell. 2002; 10:1223–33. [PubMed: 12453428]
13. Iizuka M, Stillman B. Histone acetyltransferase HBO1 interacts with the ORC1 subunit of the human initiator protein. J Biol Chem. 1999; 274:23027–34. [PubMed: 10438470]
14. Burke TW, Cook JG, Asano M, Nevins JR. Replication factors MCM2 and ORC1 interact with the histone acetyltransferase HBO1. J Biol Chem. 2001; 276:15397–408. [PubMed: 11278932]
15. Pasero P, Bensimon A, Schwob E. Single-molecule analysis reveals clustering and epigenetic regulation of replication origins at the yeast rDNA locus. Genes Dev. 2002; 16:2479–84. [PubMed: 12368258]
16. Pappas DL Jr. Frisch R, Weinreich M. The NAD(+)-dependent Sir2p histone deacetylase is a negative regulator of chromosomal DNA replication. Genes Dev. 2004; 18:769–81. [PubMed: 15082529]
17. Raghuraman MK, et al. Replication dynamics of the yeast genome. Science. 2001; 294:115–21. [PubMed: 11588253]
18. Wyrick JJ, et al. Genome-wide distribution of ORC and MCM proteins in S. cerevisiae: high-resolution mapping of replication origins. Science. 2001; 294:2357–60. [PubMed: 11743203]
19. Cheung P, et al. Synergistic coupling of histone H3 phosphorylation and acetylation in response to epidermal growth factor stimulation. Mol Cell. 2000; 5:905–15. [PubMed: 10911985]
20. Strahl BD, et al. Methylation of histone H4 at arginine 3 occurs in vivo and is mediated by the nuclear receptor coactivator PRMT1. Curr Biol. 2001; 11:996–1000. [PubMed: 11448779]
21. Zhang L, Eugeni EE, Parthun MR, Freitas MA. Identification of novel histone post-translational modifications by peptide mass fingerprinting. Chromosoma. 2003; 112:77–86. [PubMed: 12937907]
22. Ye J, et al. Histone H4 lysine 91 acetylation a core domain modification associated with chromatin assembly. Mol Cell. 2005; 18:123–30. [PubMed: 15808514]
23. Taverna SD, et al. Long-distance combinatorial linkage between methylation and acetylation on histone H3 N termini. Proc Natl Acad Sci U S A. 2007; 104:2086–91. [PubMed: 17284592]
24. Zakian VA, Scott JF. Construction, replication, and chromatin structure of TRP1 RI circle, a multiple-copy synthetic plasmid derived from Saccharomyces cerevisiae chromosomal DNA. Mol Cell Biol. 1982; 2:221–32. [PubMed: 6287231]
25. Thoma F, Bergman LW, Simpson RT. Nuclease digestion of circular TRP1ARS1 chromatin reveals positioned nucleosomes separated by nuclease-sensitive regions. J Mol Biol. 1984; 177:715–33. [PubMed: 6384525]
26. Ducker CE, Simpson RT. The organized chromatin domain of the repressed yeast a cell-specific gene STE6 contains two molecules of the corepressor Tup1p per nucleosome. Embo J. 2000; 19:400–9. [PubMed: 10654939]
27. Dean A, Pederson DS, Simpson RT. Isolation of yeast plasmid chromatin. Methods Enzymol. 1989; 170:26–41. [PubMed: 2671602]
28. Ivanov D, Nasmyth K. A topological interaction between cohesin rings and a circular minichromosome. Cell. 2005; 122:849–60. [PubMed: 16179255]
29. Craig R, Beavis RC. TANDEM: matching proteins with tandem mass spectra. Bioinformatics. 2004; 20:1466–7. [PubMed: 14976030]
30. Brewer BJ, Fangman WL. The localization of replication origins on ARS plasmids in S. cerevisiae. Cell. 1987; 51:463–71. [PubMed: 2822257]
31. Garcia BA, et al. Organismal differences in post-translational modifications in histones H3 and H4. J Biol Chem. 2007; 282:7641–55. [PubMed: 17194708]
32. Kristjuhan A, et al. Transcriptional inhibition of genes with severe histone h3 hypoacetylation in the coding region. Mol Cell. 2002; 10:925–33. [PubMed: 12419235]
33. Strahl BD, et al. Set2 is a nucleosomal histone H3-selective methyltransferase that mediates transcriptional repression. Mol Cell Biol. 2002; 22:1298–306. [PubMed: 11839797]
34. Pokholok DK, et al. Genome-wide map of nucleosome acetylation and methylation in yeast. Cell. 2005; 122:517–27. [PubMed: 16122420]

35. Carrozza MJ, et al. Histone H3 methylation by Set2 directs deacetylation of coding regions by Rpd3S to suppress spurious intragenic transcription. Cell. 2005; 123:581–92. [PubMed: 16286007]
36. Masumoto H, Hawke D, Kobayashi R, Verreault A. A role for cell-cycle-regulated histone H3 lysine 56 acetylation in the DNA damage response. Nature. 2005; 436:294–8. [PubMed: 16015338]
37. Li Q, et al. Acetylation of histone H3 lysine 56 regulates replication-coupled nucleosome assembly. Cell. 2008; 134:244–55. [PubMed: 18662540]
38. Maas NL, Miller KM, DeFazio LG, Toczyski DP. Cell cycle and checkpoint regulation of histone H3 K56 acetylation by Hst3 and Hst4. Mol Cell. 2006; 23:109–19. [PubMed: 16818235]
39. Kaplan T, et al. Cell cycle- and chaperone-mediated regulation of H3K56ac incorporation in yeast. PLoS Genet. 2008; 4:e1000270. [PubMed: 19023413]
40. Megee PC, Morgan BA, Smith MM. Histone H4 and the maintenance of genome integrity. Genes Dev. 1995; 9:1716–27. [PubMed: 7622036]
41. Megee PC, Morgan BA, Mittman BA, Smith MM. Genetic analysis of histone H4: essential role of lysines subject to reversible acetylation. Science. 1990; 247:841–5. [PubMed: 2106160]
42. Smith CM, et al. Mass spectrometric quantification of acetylation at specific lysines within the amino-terminal tail of histone H4. Anal Biochem. 2003; 316:23–33. [PubMed: 12694723]
43. Suka N, Luo K, Grunstein M. Sir2p and Sas2p opposingly regulate acetylation of yeast histone H4 lysine16 and spreading of heterochromatin. Nat Genet. 2002; 32:378–83. [PubMed: 12379856]
44. Kimura A, Umehara T, Horikoshi M. Chromosomal gradient of histone acetylation established by Sas2p and Sir2p functions as a shield against gene silencing. Nat Genet. 2002; 32:370–7. [PubMed: 12410229]
45. Tye BK. Minichromosome maintenance as a genetic assay for defects in DNA replication. Methods. 1999; 18:329–34. [PubMed: 10454994]
46. Hogan E, Koshland D. Addition of extra origins of replication to a minichromosome suppresses its mitotic loss in cdc6 and cdc14 mutants of Saccharomyces cerevisiae. Proc Natl Acad Sci U S A. 1992; 89:3098–102. [PubMed: 1557417]
47. Akiyoshi B, Nelson CR, Ranish JA, Biggins S. Quantitative proteomic analysis of purified yeast kinetochores identifies a PP1 regulatory subunit. Genes Dev. 2009
48. Hyland EM, et al. Insights into the role of histone H3 and histone H4 core modifiable residues in Saccharomyces cerevisiae. Mol Cell Biol. 2005; 25:10060–70. [PubMed: 16260619]
49. Chandrasekharan MB, Huang F, Sun ZW. Ubiquitination of histone H2B regulates chromatin dynamics by enhancing nucleosome stability. Proc Natl Acad Sci U S A. 2009; 106:16686–91. [PubMed: 19805358]
50. Fleming AB, Kao CF, Hillyer C, Pikaart M, Osley MA. H2B ubiquitylation plays a role in nucleosome dynamics during transcription elongation. Mol Cell. 2008; 31:57–66. [PubMed: 18614047]
51. Pryde F, et al. H3 k36 methylation helps determine the timing of cdc45 association with replication origins. PLoS One. 2009; 4:e5882. [PubMed: 19521516]
52. Possoz C, Filipe SR, Grainge I, Sherratt DJ. Tracking of controlled Escherichia coli replication fork stalling and restart at repressor-bound DNA in vivo. Embo J. 2006; 25:2596–604. [PubMed: 16724111]
53. Ling X, Harkness TA, Schultz MC, Fisher-Adams G, Grunstein M. Yeast histone H3 and H4 amino termini are important for nucleosome assembly in vivo and in vitro: redundant and position-independent functions in assembly but not in gene regulation. Genes Dev. 1996; 10:686–99. [PubMed: 8598296]
54. Thomas BJ, Rothstein R. The genetic control of direct-repeat recombination in Saccharomyces: the effect of rad52 and rad1 on mitotic recombination at GAL10, a transcriptionally regulated gene. Genetics. 1989; 123:725–38. [PubMed: 2693208]
55. Zhao X, Muller EG, Rothstein R. A suppressor of two essential checkpoint genes identifies a novel protein that negatively affects dNTP pools. Mol Cell. 1998; 2:329–40. [PubMed: 9774971]
56. Vincent JA, Kwong TJ, Tsukiyama T. ATP-dependent chromatin remodeling shapes the DNA replication landscape. Nat Struct Mol Biol. 2008; 15:477–84. [PubMed: 18408730]

57. Keller A, Nesvizhskii AI, Kolker E, Aebersold R. Empirical statistical model to estimate the accuracy of peptide identifications made by MS/MS and database search. Anal Chem. 2002; 74:5383–92. [PubMed: 12403597]

58. Rauch A, et al. Computational Proteomics Analysis System (CPAS): an extensible, open-source analytic system for evaluating and publishing proteomic data and high throughput biological experiments. J Proteome Res. 2006; 5:112–21. [PubMed: 16396501]

59. Liberi G, et al. Methods to study replication fork collapse in budding yeast. Methods Enzymol. 2006; 409:442–62. [PubMed: 16793417]

60. Lopes M, Cotta-Ramusino C, Liberi G, Foiani M. Branch migrating sister chromatid junctions form at replication origins through Rad51/Rad52-independent mechanisms. Mol Cell. 2003; 12:1499–510. [PubMed: 14690603]

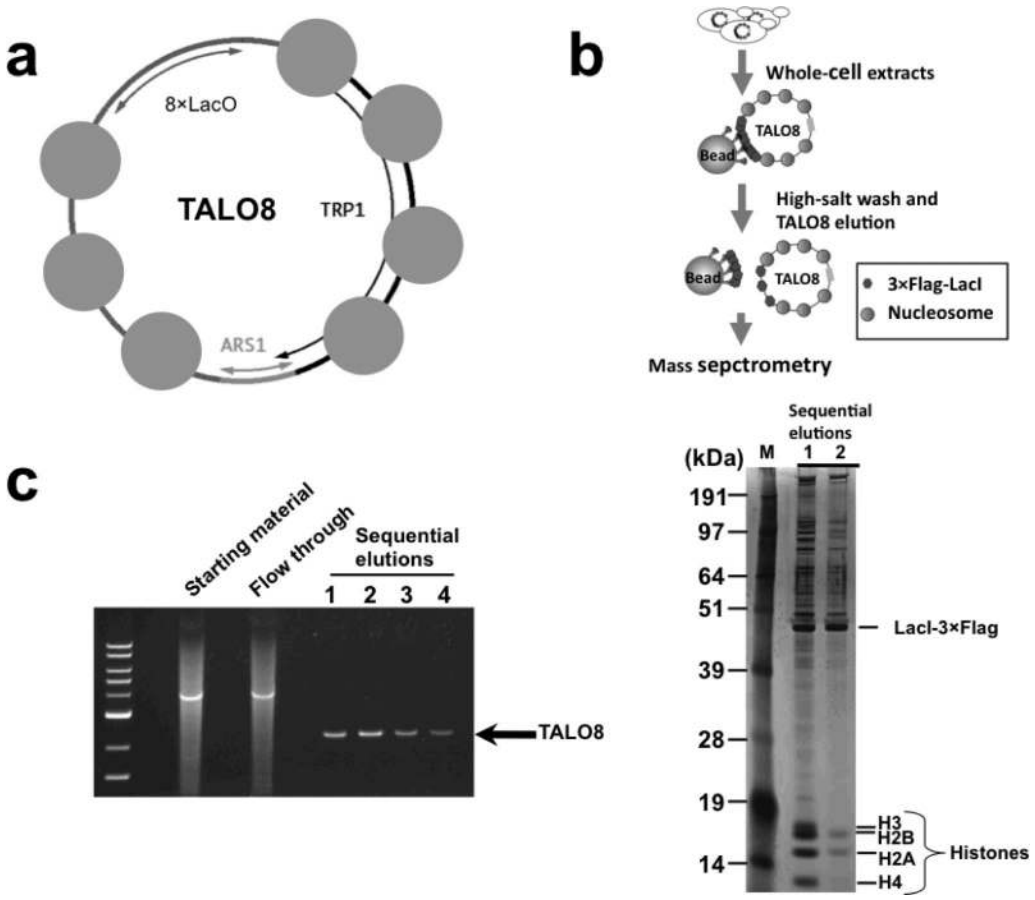

Figure 1. The TRP1-ARS1-8xLacO (TALO8) minichromosome system

(**a**) TALO8 is a ~1.8 kb minichromosome with an ARS1 origin of replication, seven well-mapped nucleosomes[25] (depicted as blue circles), a tandem array of eight lac operator sequences (8× Lac O) and a TRP1 selectable marker. (**b**) A schematic overview of the affinity-purification of TALO8. (**c**) Representative agarose gel (ethidium bromide-stained) of purified TALO8 DNA linearized by *Nhe*I (left) and silver-stained polyacrylamide gel of the purified proteins associated with TALO8 (right). The amount of samples loaded on each elution lane corresponds to 1.5×10^5 and 7.5×10^4 cell equivalents for the agarose and polyacrylamide gels respectively. Typically, eluates 1 and 2 were pooled and prepared for mass spectrometry.

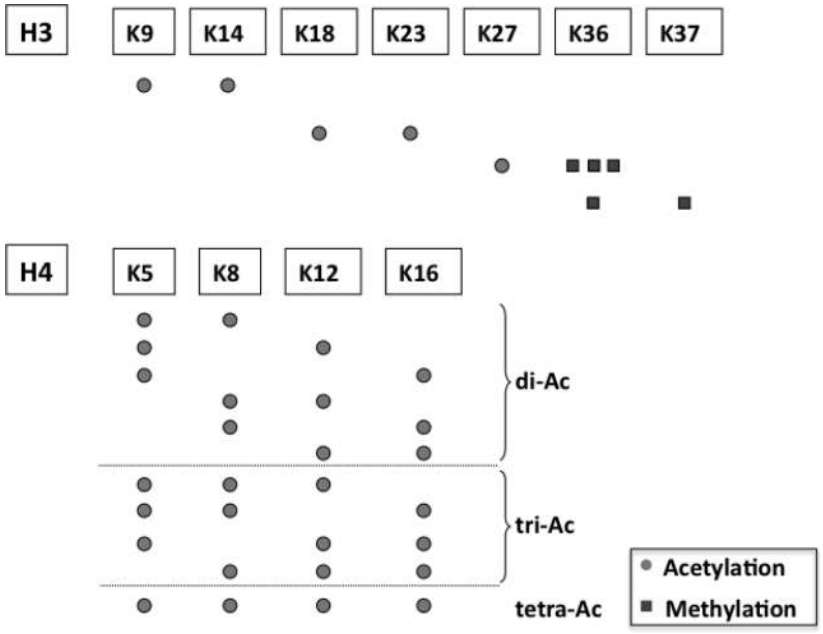

Figure 2. Identification of combinations of modifications occuring on the same peptide in TALO8 histones

Combinations of histone modifications detected on the same peptide from histones H3 and H4 on TALO8 are shown on the same horizontal row. For lysine methylations, the number of squares indicates the level of methylation.

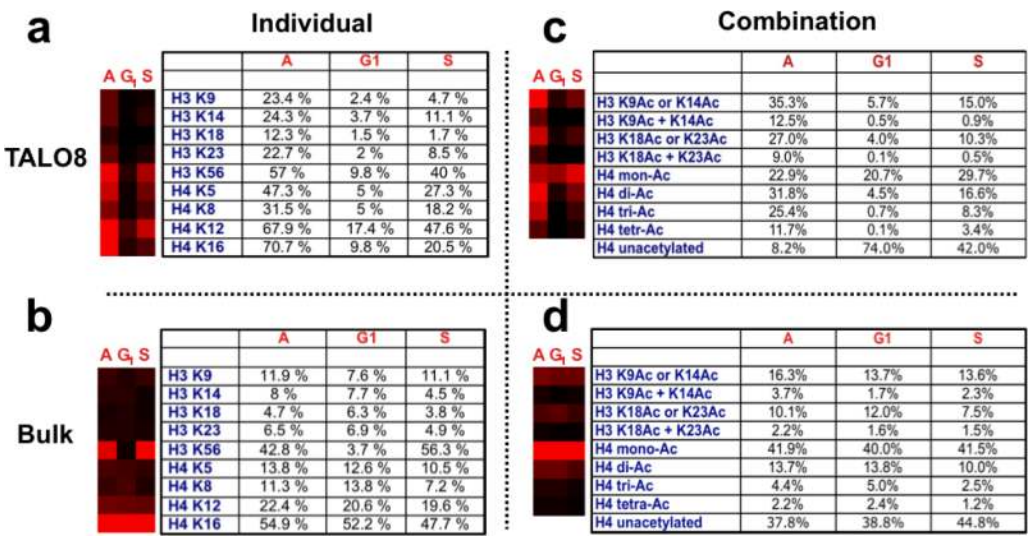

Figure 3. Quantitative analysis of histone acetylations

(**a**) Quantitative analysis of histone acetylations per indicated lysine residue of TALO8-purified histones H3 and H4. Histone acetylation at individual lysines are scored independently of the acetylation states of other lysines. The table indicates the absolute level (in percentage) of histone acetylation detected for each of the indicated residues over the course of the cell cycle. The quantitative data is graphically represented using TreeView, and the intensity of red indicates increasing abundance. "A" refers to asynchronously growing cells. The S phase samples were prepared at 17 minutes after release from α-factor, as done for Figure 2. (**b**) Quantitative analysis of histone acetylation per lysine residue, as in (**a**), but on bulk, chromatin-bound histones. (**c**) Quantitative analysis of combinations of histone acetylations present on TALO8 purified histones. Analysis was done as in (A), with the absolute levels shown in the table and a graphical representation on the left. "H3 K9Ac or K14Ac" indicates peptides containing a single acetyl group which was present either on H3 K9 or H3 K14. Alternatively, "H3 K9Ac K14Ac" indicates di-acetylated peptides where both K9 and K14 were acetylated. The notation is the same for the peptide containing H3 K18 and K23. In the case of histone H4, mono-acetylated amino-terminal peptides (containing K5, K8, K12 and K16) are denoted as "H4 mono Ac", di-acetylated peptides are "H4 di Ac", tri-acetylated peptides are "H4 tri Ac" and peptides where K5, K8, K12 and K16 are all acetylated are "H4 tetra Ac". "A" refers to asynchronously growing cells. The S phase samples were prepared at 17 minutes after release from alpha factor, as done for Figure 2. (**d**) Quantitative analysis of combinations of histone acetylations, as in (**c**), but on bulk, chromatin-bound histones.

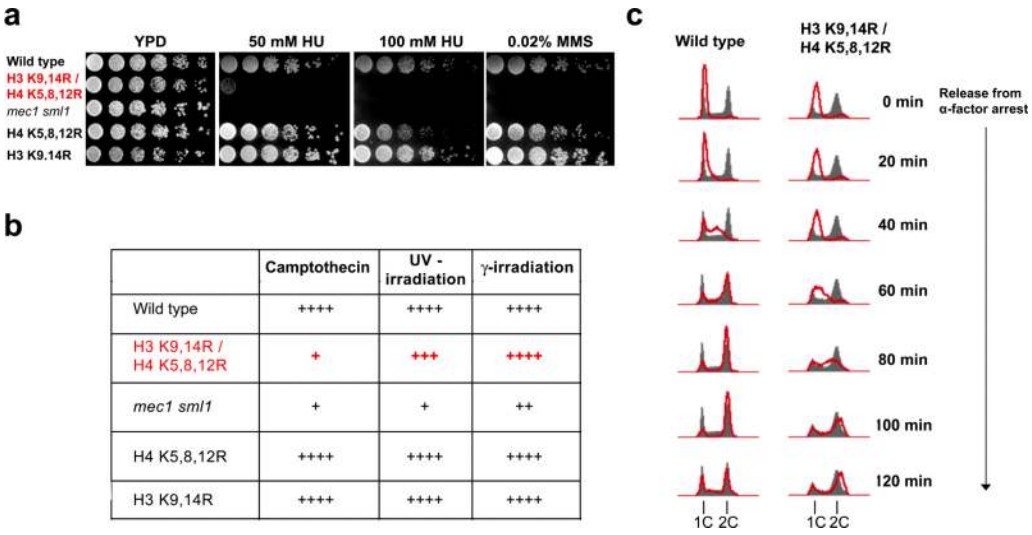

	Camptothecin	UV - irradiation	γ-irradiation
Wild type	++++	++++	++++
H3 K9,14R / H4 K5,8,12R	+	+++	++++
mec1 sml1	+	+	++
H4 K5,8,12R	++++	++++	++++
H3 K9,14R	++++	++++	++++

Figure 4. Acetylation of multiple lysine residues on histone H3 and H4 tails is required for efficient DNA replication

(**a**) The histone acetylation mutant is hypersensitive to drugs that cause replication stress. Five-fold serial dilutions of yeast strains were spotted onto YPD plates containing 50mM hydroxyurea (HU), 100mM HU, 0.02% methyl methanesulfonate (MMS) or YPD alone and grown at 25°C for 4 days. (**b**) The histone acetylation mutant is specifically sensitive to replication stress. Sensitivity of the cells was tested against other forms of DNA damage and is indicated from most resistant (++++) to most sensitive (+). (**c**) The histone acetylation mutant exhibits delayed S-phase progression. Asynchronous cultures of wild type or mutant cells were pre-synchronized in G1 with α-factor at 25°C in YPD. Cells were filtered, washed and released into fresh YPD medium containing 0.1mg/ml Pronase E. Samples were collected at the indicated time points and analyzed by FACS. The grey signals show the FACS profiles of asynchronous culture, and the red lines denote the arrest/release kinetics.

a

	Rate of minichromosome loss (%)	
	ARS1 + 7X mutARS209	ARS1 + 7XARS209
Wild type	1.9 ± 0.5	1.8 ± 1
Histone mutant	18.2 ± 2	3.8 ± 0.6

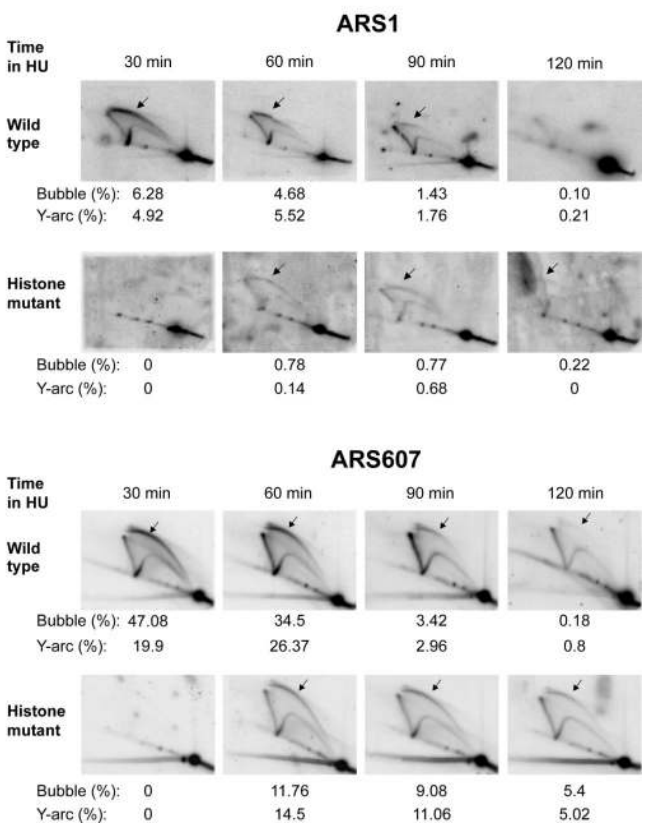

Figure 5. Acetylation of multiple lysine residues on H3 and H4 tails facilitates origin firing

(**a**) The histone acetylation mutant has an elevated plasmid loss rate. Plasmids containing a functional ARS1 and seven copies of either functional (pDK368-7, right) or mutant ARS209 (pDK398-7, left) were transformed into the histone acetylation mutant and wild type control, and their loss rates were measured as described previously[46]. The numbers denote the mean and the standard deviation of the plasmid loss rates (%) per generation. (**b**) 2-D agarose gel analyses indicate that the histone mutant is deficient in origin firing. Wild type and histone mutant cells were grown in YPD medium, pre-synchronized in G1 with α-factor at 25°C and released into fresh medium containing 200mM hydroxyurea (HU) and 0.1mg/ml Pronase E. DNA was prepared from cells harvested at the indicated times, digested with *Nco*I and subjected to electrophoresis in two dimensions. The DNA was transferred onto nylon membranes and probed with a ^{32}P-labelled DNA fragment spanning the ARS1 origin. Quantitation of the abundance of bubble intermediates (indicated by arrows) and Y-arcs as a percentage relative to the 1N spot is given below each image. A schematic representation of relevant replication intermediates is also shown. (**c**) 2-D agarose gel analyses of another early, efficient origin, ARS607, indicate deficient origin firing in the histone mutant. DNA was digested with *BspH*I and *Cla*I and analyzed as in (**b**), using a ^{32}P-labelled DNA fragment spanning ARS607. Relative quantitation of the replication intermediates (as percentage of the 1N spot intensity) is shown, as in (**b**).

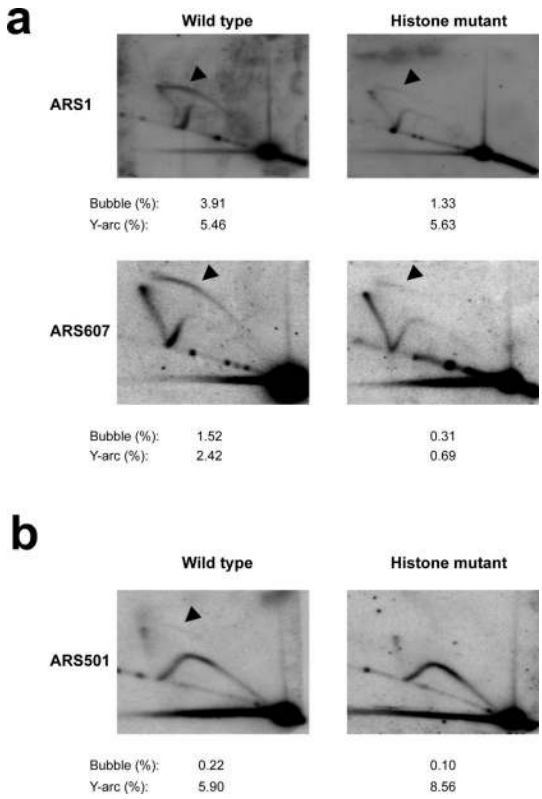

Figure 6. Acetylation of multiple lysine residues on H3 and H4 tails facilitates origin firing during normal growth

(**a**) 2-D agarose gel analyses of early origins in the histone mutant under unperturbed growth conditions indicate deficient origin firing. DNA was prepared from pooled S-phase populations of wild type or histone mutant cells, as in Fig 5. *Nco*I (ARS1) or *BspH*I *Cla*I (ARS607) digested DNA was subjected to 2-D gel analyses as before. Relative quantitation of bubble intermediates (represented by arrowheads) and Y-arcs is shown below (as percentage of the 1N spot intensity). (**b**) Pooled S-phase DNA from (**a**) was digested with *Xba*I and subject to 2-D gel analyses. A relative quantitation of bubble intermediate (represented by an arrowhead) and Y-arcs is presented below (as percentage of the 1N spot intensity).